Combined Megavoltage and Contrast-Enhanced Radiotherapy as an Intrafraction Motion Management Strategy in Lung SBRT

Daniel A. Coronado-Delgado, MSc[1] and
Héctor M. Garnica-Garza, PhD[2]

Abstract

Using Monte Carlo simulation and a realistic patient model, it is shown that the volume of healthy tissue irradiated at therapeutic doses can be drastically reduced using a combination of standard megavoltage and kilovoltage X-ray beams with a contrast agent previously loaded into the tumor, without the need to reduce standard treatment margins. Four-dimensional computed tomography images of 2 patients with a centrally located and a peripherally located tumor were obtained from a public database and subsequently used to plan robotic stereotactic body radiotherapy treatments. Two modalities are assumed: conventional high-energy stereotactic body radiotherapy and a treatment with contrast agent loaded in the tumor and a kilovoltage X-ray beam replacing the megavoltage beam (contrast-enhanced radiotherapy). For each patient model, 2 planning target volumes were designed: one following the recommendations from either Radiation Therapy Oncology Group (RTOG) 0813 or RTOG 0915 task group depending on the patient model and another with a 2-mm uniform margin determined solely on beam penumbra considerations. The optimized treatments with RTOG margins were imparted to the moving phantom to model the dose distribution that would be obtained as a result of intrafraction motion. Treatment plans are then compared to the plan with the 2-mm uniform margin considered to be the ideal plan. It is shown that even for treatments in which only one-fifth of the total dose is imparted via the contrast-enhanced radiotherapy modality and with the use of standard treatment margins, the resultant absorbed dose distributions are such that the volume of healthy tissue irradiated to high doses is close to what is obtained under ideal conditions

Introduction

Tumor intrafraction motion represents perhaps the most serious impediment to fully exploiting the recent innovations in technology and treatment strategies in the field of radiotherapy. Traditionally, the most straightforward and perhaps most widely available solution to this problem has been the use of generous treatment margins such that the gross target volume (GTV) is fully encompassed by the radiation beam, regardless

[1] Centro de Investigacion y de Estudios Avanzados Unidad Monterrey Apodaca, Nuevo León, Mexico
[2] CINVESTAV IPN Via del Conocimiento 201 Parque PIIT Ciudad de Mexico, Mexico

Corresponding Author:
Héctor M. Garnica-Garza, 2CINVESTAV IPN Via del Conocimiento 201 Parque PIIT Ciudad de Mexico, 07360 Mexico.
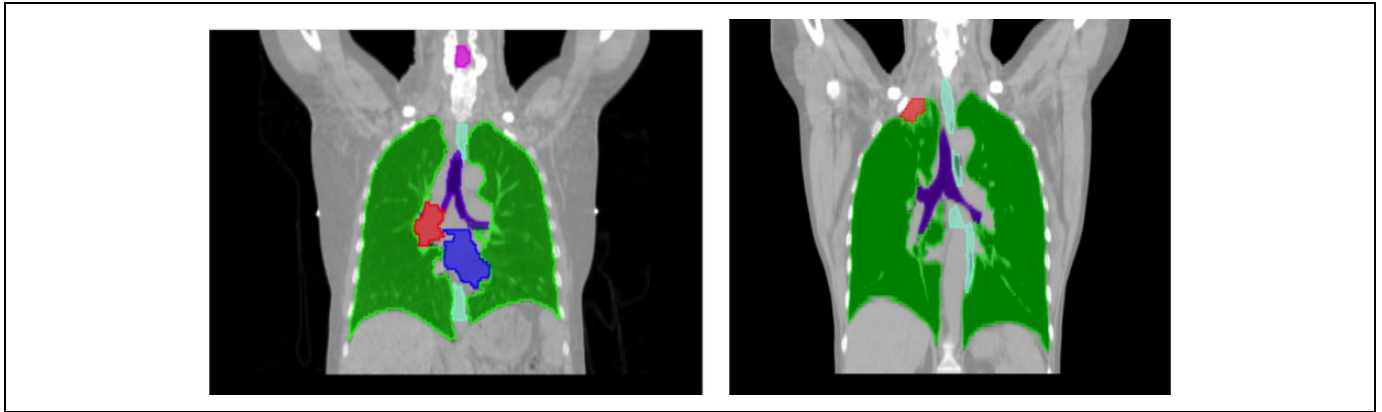Email: hgarnica@cinvestav.mx

Figure 1. Coronal views of the 2 patient models used in this work. Several relevant structures were already contoured, including the gross target volume (GTV), both lungs, heart, and trachea.

of its position in the motion cycle.[1] This solution carries the obvious disadvantage that large volumes of healthy tissue, the planning target volume (PTV), are irradiated to the same absorbed dose level as the GTV itself. To address this shortcoming and try to reduce the treatment margins, several technologies have been implemented which are capable of monitoring in real time the position of the GTV. These technologies can be classified into 2 broad categories: static synchronized delivery and dynamic radiologic tumor tracking. Among the former, respiratory gating relies on the use of a breathing monitor placed on the patient surface and usually optical in nature. The motion of the GTV is assumed to correlate with that of the breathing monitor, and only when the latter is in a position previously determined as suitable to carry out the treatment, the radiation beam is turned on. This effectively synchronizes the treatment delivery to the respiratory cycle.[2] One problem with this approach is that the internal position of the target must be inferred from surface motions. Another problem is the reduced efficiency, as the overall treatment time is increased. Dynamic tumor tracking, on the other hand, aims to alleviate these problems by continuously monitoring the target position during the irradiation, either using sets of radiological images,[3] 2 at least, or a combination of a single image and a target motion model.[4,5] By continuously monitoring the location of the GTV, adjustments to the position and direction from which the radiation beam is aimed to the target are made in order to account for the GTV motion. While these technologies represent state-of-the-art solutions to the intrafraction motion problem, they introduce an extra layer of complexity to the already challenging problem posed by the irradiation of an internal structure with what for practical purposes is an invisible radiation beam. From this perspective, the simplicity of the generous margin strategy remains unrivaled, and therefore it is worth exploring techniques that might lead to its improvement with regard to the large amount of healthy tissue irradiated to therapeutic doses without resorting to the minimization of the PTV itself. In this context, we hypothesize that if the radiation absorption properties of the GTV were somehow modified in order to create a larger dose difference with respect to the

surrounding tissue, the size of the PTV margin could be kept as large as the motion amplitude would dictate, as the surrounding tissue would never reach the same dose level as the GTV. This is precisely the rationale behind contrast-enhanced radiotherapy (CERT),[6,7] where a radiological contrast agent previously loaded into the tumor, where it tends to accumulate, enhances the absorption of X-rays at the kilovoltage energy range, thus creating a large dose gradient between the GTV and the surrounding tissues.

In this work, we will indeed show that a stereotactic body radiotherapy (SBRT) lung treatment with recommended PTV margins can be dramatically improved and that in fact can be made to resemble what would be obtained under ideal conditions of no tumor movement and minimum PTV margin by imparting a fraction of the total dose under the CERT treatment scheme.

Materials and Methods

Patient Models

For this study, 2 patient models, both with non-small cell lung tumors, were obtained from The Cancer Imaging Archive[8-10] in the form of 4-dimensional computed tomography (4DCT) images with 10 breathing phases. The resolution of these 4DCT images is 1×1 mm with a slice thickness of 3 mm, and the GTV, lungs, heart, and other major structures were already segmented at each phase in the respiratory cycle. Patient model A presents a centrally located GTV in the right lung having a volume of 30.3 cm³. Patient model B on the other hand has a peripherally located GTV with a volume of 31.1 cm³. This second model in particular was chosen as a portion of the ribs, highly efficient in absorbing kilovoltage X-ray beams, is located near the GTV in such a way that the PTV overlaps with it. Coronal views of both models are shown in Figure 1. As the skin and bone structures are also of interest for our purposes, a separate software, 3D Slicer (www.slicer.org), was used to delineate the skin, ribs, and sternum on the whole set of 4DCT images. Following the recommendations of RTOG 0813 and RTOG 0915, the PTV margins for both the patients were
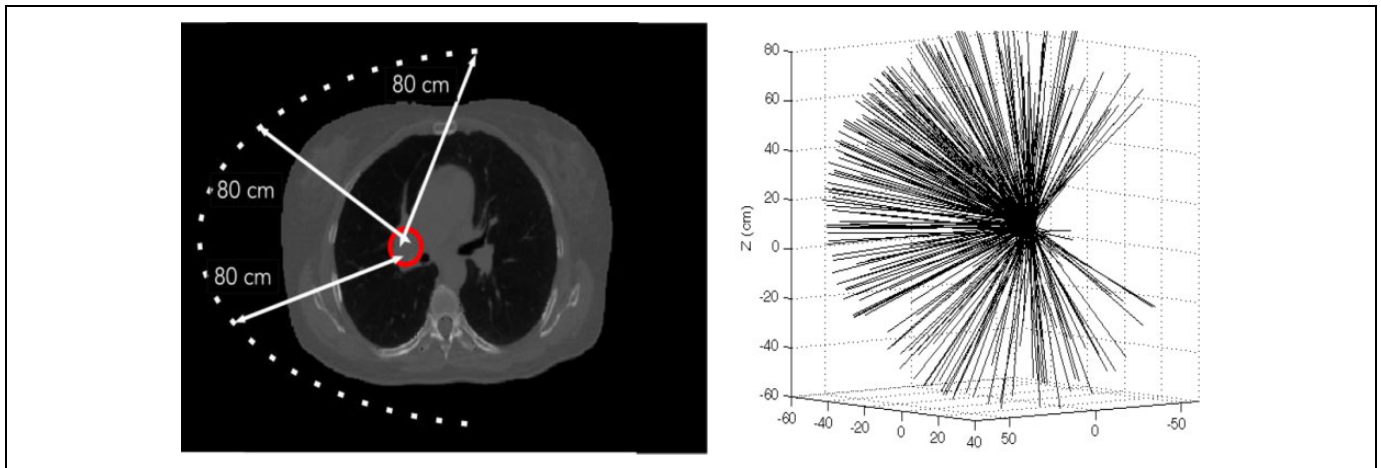
Figure 2. Irradiation setup for the treatment plans modeled in this work. A semispherical shell with 80-cm radius from the geometric center of the gross target volume (GTV) was used to lay a grid of dwell positions. The right panel shows actual irradiation points and directions. The geometric center of the tumor is located at 5.7, 15.3, and 17.0 cm.

contoured directly around the GTV and having dimensions of 1 cm in the craniocaudal direction and 0.5 cm in the lateral direction.[11,12] In order to simulate an ideal treatment, that is, a treatment in which there is no intrafraction motion, and therefore the PTV margin can be as small as the beam penumbra will allow, separate patient models were generated with PTV margins of 2 mm in all directions using only the CT images obtained at the deep inspiration stage. While an average image over the whole set of 4DCT images would perhaps be a more appropriate representation, this resulted in blurred organs and structures.

Treatment Planning

It is assumed that the treatment is delivered under conditions of robotic SBRT.[3] A total of 300 circular beams with a 2 cm diameter for patient model A and 1 cm diameter for patient model B were used for each treatment, and each beam could be turned on and off by the optimization algorithm, described below. These diameters were selected after comparing treatments with different beam sizes. A separate software was used to determine the irradiation points and orientation for each beam, tailored to each patient model, as described previously.[13] Only ipsilateral irradiations were allowed in order to minimize the unnecessary exposure of healthy tissue and the same irradiation points and directions were used for both the high-energy and the CERT treatments. Figure 2 shows the irradiation setup for one of the treatment cases examined in this work. For each patient model, the following plans were calculated, in all cases using the deep inspiration CT images:

1. A CyberKnife-like ideal treatment plan with a uniform PTV margin of 2 mm. This was the minimum possible margin without degrading the absorbed dose distribution in the GTV. This plan served as the reference plan.
2. A high-energy treatment plan with the PTV margin as recommended by the RTOG 0813 protocol.

3. A CERT plan with the margin recommended in RTOG 0813 and RTOG 0915.
4. A set of plans combining the treatment plans 2 and 3 mentioned earlier with different proportions of the total prescribed dose imparted by each modality, from 80% MV to 20% CERT to 50% of the prescribed dose by each modality

Each of these plans was optimized according to the same set of prescription goals as recommended in either RTOG 0813 or RTOG 0915 and listed in Table 1. The simultaneous projection feasibility algorithm of Cimmino[14] was used to carry out the optimization. The application of this algorithm in radiotherapy is described in Censor et al,[15] and our implementation has been discussed before.[13]

Absorbed Dose Calculations

Conversion from Hounsfield units to material composition. In order to define the different materials present in the patient model, a calibration curve that converts CT numbers into elemental weight data using 12 different materials as the basis was used.[16] Computer scripts were developed to read the CT images, convert the voxel data into its respective material type, and write the corresponding files in the format needed by the Monte Carlo code, described below. The material representing the contrast agent embedded in the tumor tissue was treated separately, as it is not actually present in the patient models used: It is assumed that the contrast agent is based on gold nanoparticles (GNP)[6] and that its concentration in the GTV is 10 mg-Au/g, a concentration deemed feasible.[17] The tumor is assumed to consist of soft tissue with the weight fraction of each material adjusted to incorporate gold at the concentration stated earlier. The contrast agent was assumed to be present both in the high-energy and the CERT treatment, although in the former it resulted in no discernible effect.

Table 1. Prescription Goals Used in the Optimization of the Treatment Plans.[a]

Structure	D_{LOW}, Gy	D_{UP}, Gy	Weight
GTV	50	75	0.30
PTV	50	75	0.55
Right Lung	0	28	0.05
Heart	0	20	0.03
Esophagus	0	20	0.02
Trachea	0	25	0.05

Abbreviations: GTV, gross target volume; PTV, planning target volume.
[a]D_{LOW} and D_{UP} refer to the minimum and maximum dose limits imposed to each structure.

Table 2. Relevant Monte Carlo Information Per TG-268.

Parameter	Value
Monte Carlo code	PENELOPE-2006
Cross-sections	Built-in analytical models and tabulated data
Transport parameters	$E_{ab} = 10$ keV (photons and electrons); C1 = C2 = 0.1; $W_{cc} = W_{cr} = 100$ eV
Statistical uncertainty	2% on average for those voxels receiving at least 50% of the maximum dose

Monte Carlo simulations. The Monte Carlo code PENELOPE[18] and its accompanying set of subroutines from the PenEasy implementation[19] were used to carry out all the absorbed dose calculations reported in this work. Separate calculations were run for each of the 300 beams participating in the 2 modeled treatments. In order to determine the impact of the intrafraction motion, the absorbed dose imparted by each beam was calculated at every phase of the respiratory cycle; therefore, for each beam energy and treatment, a total of 3000 dose matrices were obtained. Following the recommendations of Task Group 268,[20] the relevant description of the software and transport parameters is shown in Table 2. The CERT treatment was imparted using a 220-kVp X-ray beam produced by a tungsten target and filtered by 2 mm of copper, while the megavoltage beam model was taken from the literature, and it is based on the Monte Carlo modeling of a CyberKnife treatment machine.[21] Our full implementation of both X-ray sources into the PENELOPE software has been detailed before.[13] X-rays of 220 kVp were used as we have previously shown that a X-ray beam with 220-kVp spectrum is an optimal compromise between penetration at depth and sizable fluence in the energy interval that maximized the absorption of the incident beam by the GNPs.[22]

Incorporation of the Effect of Intrafraction Tumor Motion Into the Treatment Delivery

In order to determine the effect that the intrafraction motion has on the resultant absorbed dose distributions for the calculated treatment plans, the optimized plans were imparted to the moving phantom at each stage in the respiratory cycle. This is done by calculating the dose distribution from each of the 300 beams, weighted according to the optimization results and adding the dose matrices. Note that, as the beams would be sequentially delivered, we would have to know in advance the particular sequence in which the patient is irradiated. To avoid this problem and make our conclusions as general as possible, each of the 10 moving phantoms was irradiated with the 300 beams, and it was then assumed that each stage in the breathing cycle received an equal proportion, one-tenth, of the total prescribed dose. The treatments thus obtained will be referred to as the imparted treatments.

Dose Accumulation Through the Motion Cycle

The open source medical image informatics software 3D Slicer was used to perform B-spline deformable image registration throughout the whole respiratory cycle (www.slicer.org). Separate computer scripts were implemented to read the vector field output files yielded by 3D Slicer and use them to correlate voxel indices among the CT images at each stage in the respiratory cycle. This correlation in turn was used to add the dose matrices as yielded by PENELOPE and our optimization software for each of the treatments modeled in this work.

Results

Patient Model A

Isodose curves on the coronal plane are shown in Figure 3 for each treatment modeled in this work, namely, ideal 6 MV and imparted, that is, accounting for intrafraction motion, 6-MV, and CERT treatments. Note that for the ideal high-energy treatment, the 30-Gy isodose curve almost spills into the contralateral lung, something that does not occur for the CERT-imparted treatment. In general, the isodose curves for the CERT treatment, in spite of patient motion, are more tightly wrapped around the GTV.

Figure 4 shows the cumulative dose–volume histogram (cDVH) for the target volumes resulting from the imparted high-energy treatment plan, in the left panel, and for the CERT plan on the right panel.

The cDVHs for the ideal megavoltage treatment are shown as a reference. As can be seen from this figure and regardless of patient motion, 95% of the PTV and 100% of the GTV receives the prescribed dose of 50 Gy, which is basically the purpose of the treatment margin recommended in RTOG 0813. While the dose distribution in the PTV is similar among the ideal and imparted treatment, it must be kept in mind that the ideal margin is smaller than the margin recommended by RTOG 0813. The ideal treatment of course also offers an appropriate target coverage but with the obvious advantage of a total PTV about half that recommended by the RTOG 0813 protocol. Table 3 shows the lung volume, including both lungs, irradiated to at least 2 particular maximum dose levels as stated in RTOG 0813. In all cases and regardless of the treatment modality, the
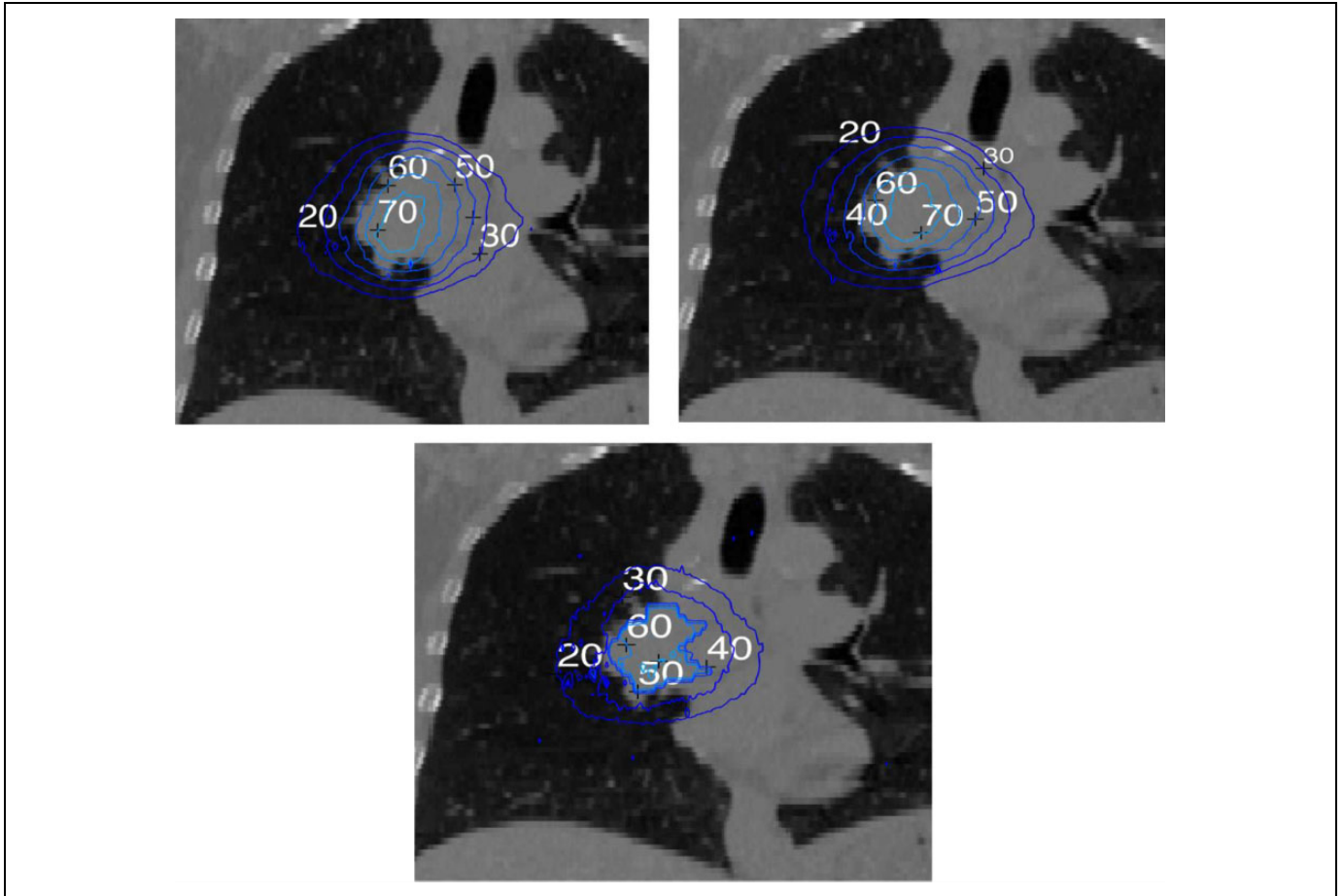
Figure 3. Isodose curves on the coronal plane for the 3 treatments modeled in this work: upper left panel—ideal 6 MV treatment; right panel—imparted 6 MV; and bottom panel—imparted contrast-enhanced radiotherapy (CERT).
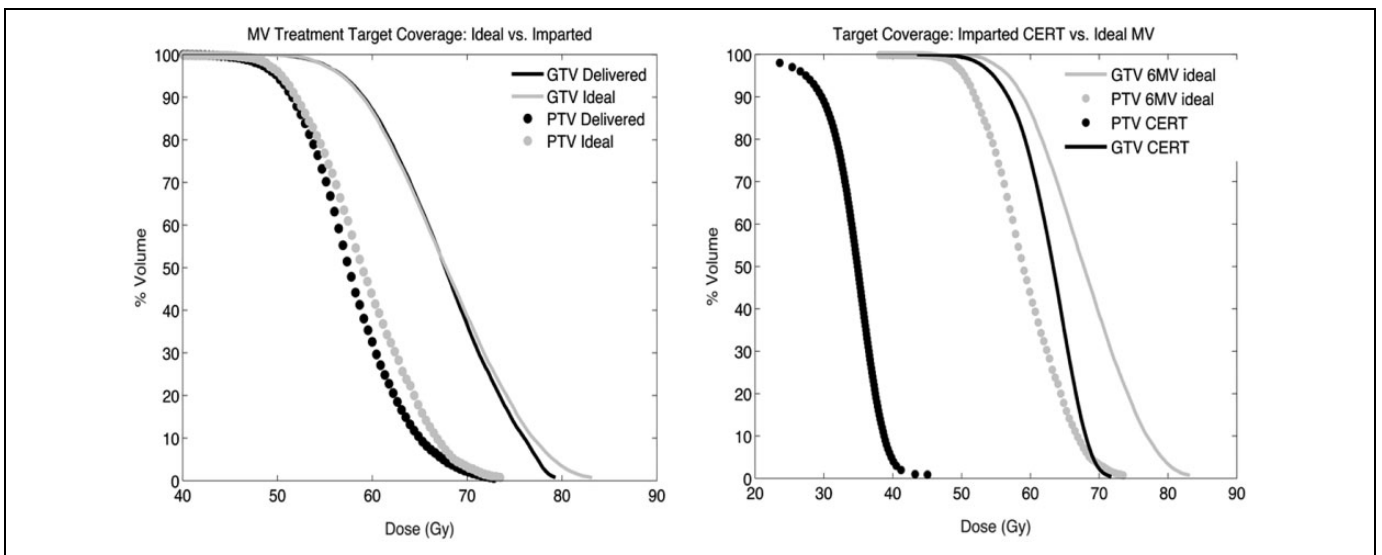

Figure 4. Cumulative dose-volume histogram (cDVHs) for the imparted treatment plans in each of the modalities modeled in this work. Target coverage in each treatment adheres to the recommendations set forth in RTOG 0813.

Table 3. Total Lung Volume (cm^3) Irradiated to at Most 12.5 Gy and 13.5 Gy.[a]

Dose	Ideal 6 MV	Imparted 6 MV	Imparted CERT
12.5 Gy	390.6	440.5	322.6
13.5 Gy	319.8	367.2	242.3

Abbreviation: CERT, contrast-enhanced radiotherapy.
[a]Both lungs are included. RTOG 0813 recommended limit at each dose level is 1000 cm^3.

Table 4. Maximum Absorbed Dose (Gy) Imparted to at Least 1 cm^3 of Selected Irradiated Structures.[a]

Structure	Ideal 6 MV	Imparted 6 MV	Imparted CERT	RTOG 0813
Lung	22.7	24.6	19.5	-
Heart	18.3	22.3	16.0	34.0
Trachea	15.7	16.0	10.0	34.8
Esophagus	10.7	12.3	8.1	30.0
Skin	6.4	6.6	16.2	36.0
Ribs	12.8	14.6	21.6	40.0

Abbreviation: CERT, contrast-enhanced radiotherapy; PTV, planning target volume.
[a]This does not consider the 2-cm margin around the PTV as specified by RTOG 0813.

irradiated critical volumes are well below the 1000 cm^3 limit stated in the said protocol.

Table 4 shows the maximum absorbed doses imparted to at least 1 cm^3 of several irradiated organs at risk (OAR) by each treatment modality along with the recommended limits for the 50-Gy dose arm of the protocol, which again regardless of the treatment modality are never exceeded. All 3 treatment plans are therefore acceptable from a clinical perspective.

Figure 5 shows the effect of combining the high-energy and CERT-imparted treatments with various weights. The GTV coverage, shown in the right panel, is not affected as expected, since the RTOG 0813 treatment margins are large enough to account for tumor motion. Note however that the cDVH curve for the PTV, shown in the right panel of Figure 5, steadily shifts toward lower dose values, as the percentage of the total dose imparted via the CERT treatment is increased. As an example, imparting 40% of the total dose via the CERT modality reduces by more than half the volume of lung tissue receiving at least 55 Gy.

Figure 6 shows the total volume receiving a dose of at least 45 Gy, 50 Gy, and 55 Gy as a function of the percentage of the total dose delivered by each modality. At the higher dose level even imparting one-fifth of the total dose with the CERT modality results in a treatment volume irradiated at 55 Gy that is on par with what is obtained under ideal conditions of no tumor movement and minimum PTV margin, although the RTOG PTV volume is larger than the ideal margin. At lower dose levels, the reduction in the total volume irradiated is not as drastic as observed at higher doses, but nevertheless a favorable change is clearly discernible.

The same trend is observed for other structures, such as the lungs and heart, as shown in Figure 7. For the lungs in particular, reductions in the total volume receiving at least 15 Gy ranges from 10% to 25% for the combinations of megavoltage and CERT treatments examined in this work. Although the change in the heart volume irradiated at a given dose level, 10 Gy for the plot in the right panel of Figure 7, is less pronounced, a downward trend is clearly discernible. It must be kept in mind that all this is happening without affecting the coverage of the GTV as previously shown in Figure 5 and with the use of standard PTV margins which ensure that the GTV is fully covered regardless of its position in the motion cycle.
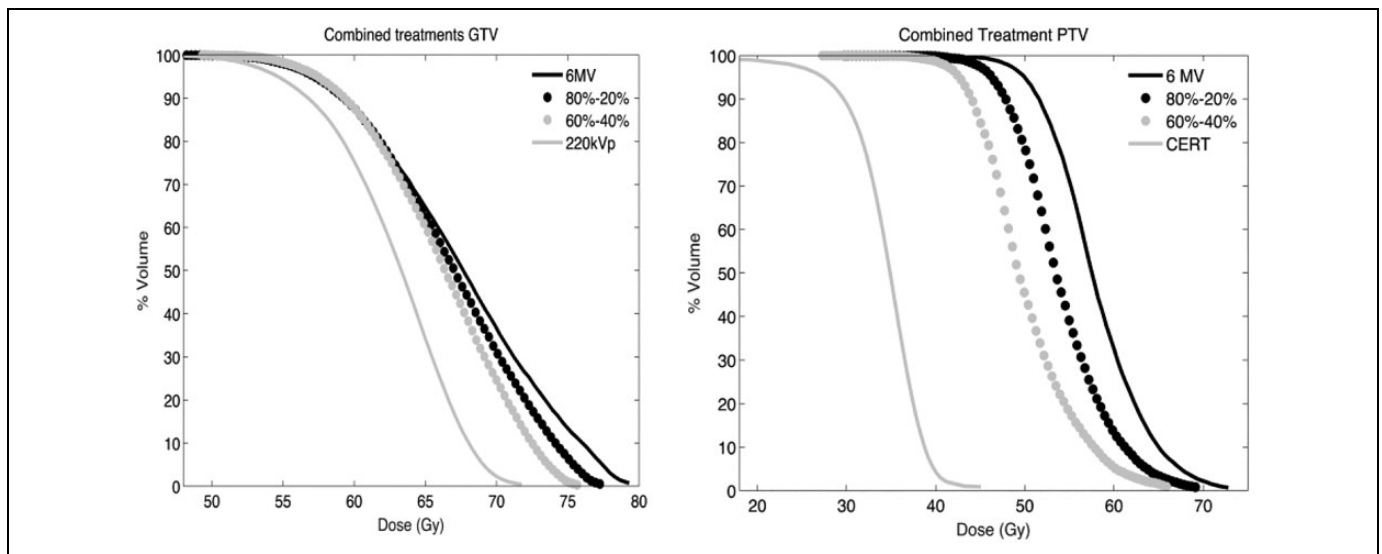

Figure 5. Cumulative dose-volume histogram (cDVHs) for the gross target volume (GTV), right panel, and PTV for different combination of high-energy and contrast-enhanced radiotherapy (CERT) treatments. Each pair of percentage figures in the labels refer to the weights of the megavoltage and the CERT treatments in this order.
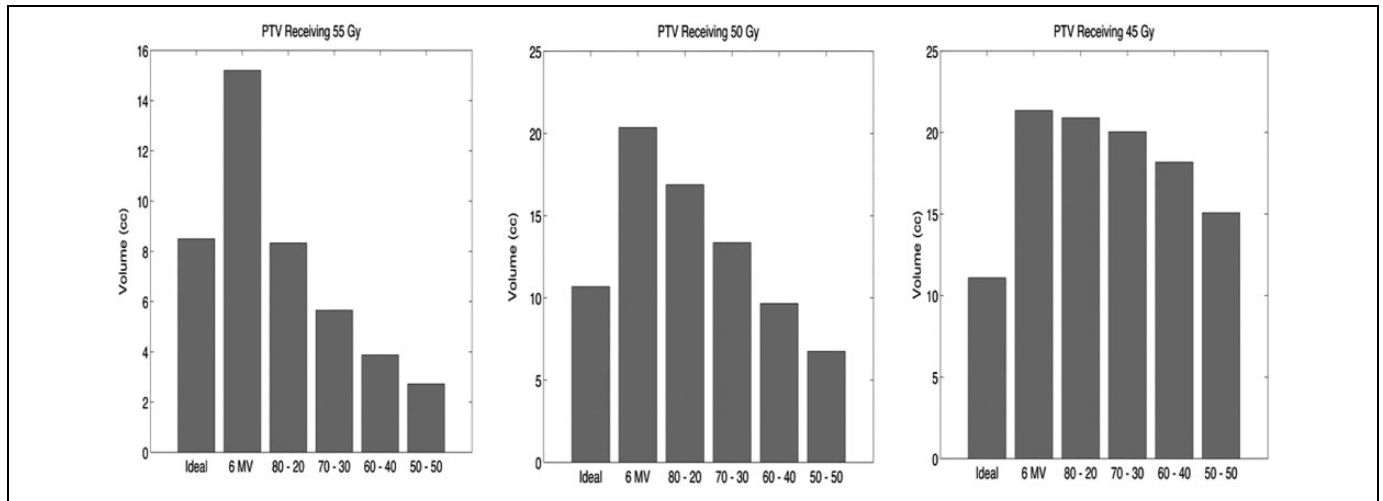
Figure 6. Total planning target volume irradiated to at least 55 Gy, 50 Gy, and 45 Gy. In these and subsequent graphs, the set of 2 numbers separated by a dash indicate the percentage of absorbed dose imparted by the high-energy and contrast-enhanced radiotherapy (CERT) modalities in this order.
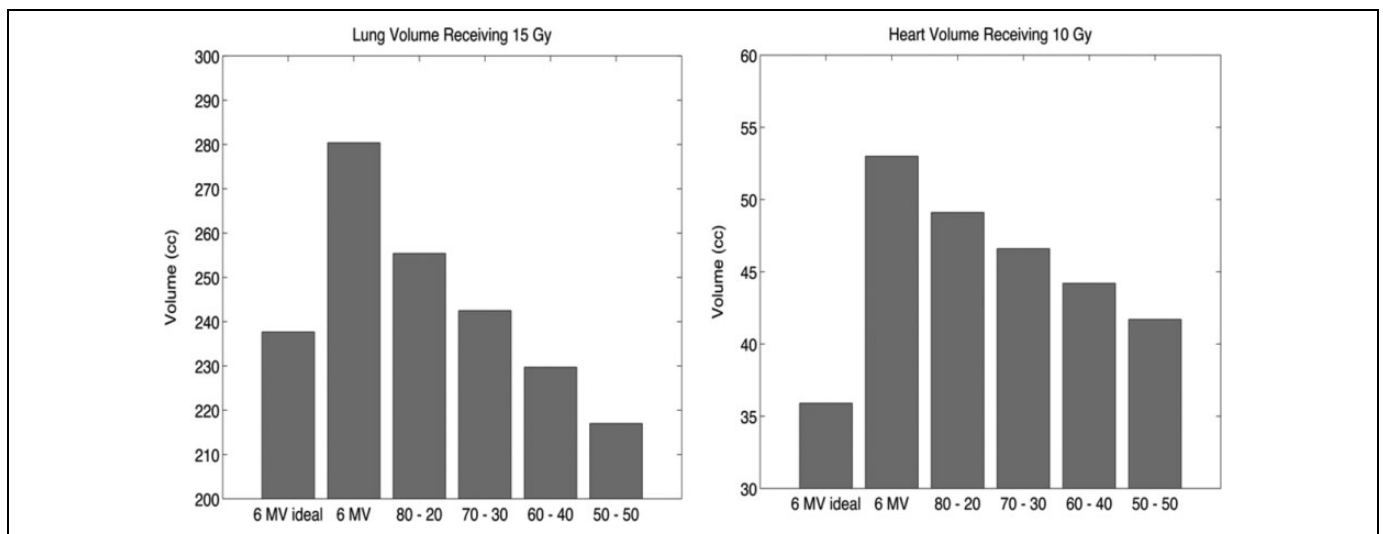

Figure 7. Left panel: total volume of lung receiving at least 15 Gy, including both lungs; right panel: volume of heart irradiated to at least 10 Gy. The 2 numbers separated by a dash on the x-axis indicate the percentage of absorbed dose imparted by the high-energy and contrast-enhanced radiotherapy (CERT) modalities, respectively.

Perhaps most important, no assumptions regarding the knowledge of the particular position of the GTV in the motion cycle are made. By combining a megavoltage and a CERT treatment, even with a modest fraction of the total dose imparted by the latter modality, we are able to obtain a treatment plan that closely resembles what would be obtained under ideal conditions of no tumor motion and beam penumbra-determined PTV margin.

On the other hand, as shown in Figure 8, the volume of skin and ribs irradiated to a given level of absorbed dose increases as the fraction of the total dose delivered by CERT increases. For the skin in particular, splitting the total dose at 80% to 20% ratio between the high-energy and CERT modalities, respectively, almost doubles the skin volume irradiated at 5 Gy. It should be pointed out however that, as shown in Table 3, even

if 100% of the prescribed dose was imparted via the CERT modality, the maximum skin dose would not exceed the RTOG 0813 stated limit of 36 Gy. The same applies to the ribs, whose maximum dose is well below the 40 Gy limit stated in the RTOG protocol. These are simply the negative consequences of the depth dose characteristics and interaction physics of kilovoltage X-ray beams that are, however, greatly reduced when combining CERT and high-energy irradiations in a single treatment strategy.

Patient Model B

Figure 9 shows isodose curves on the coronal plane for the 3 treatments modeled, namely, 6 MV ideal, 6 MV imparted,
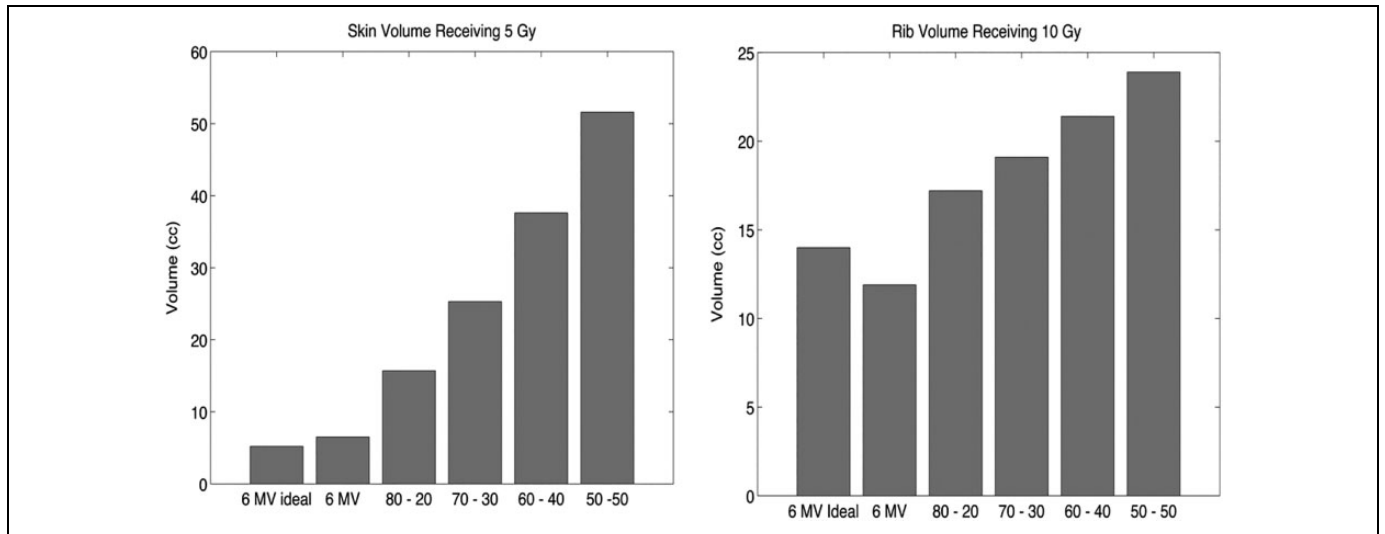
Figure 8. Volume of skin and ribs irradiated at doses of 5 Gy and 10 Gy, respectively, as a function of the total dose fraction imparted with high-energy and contrast-enhanced radiotherapy (CERT).
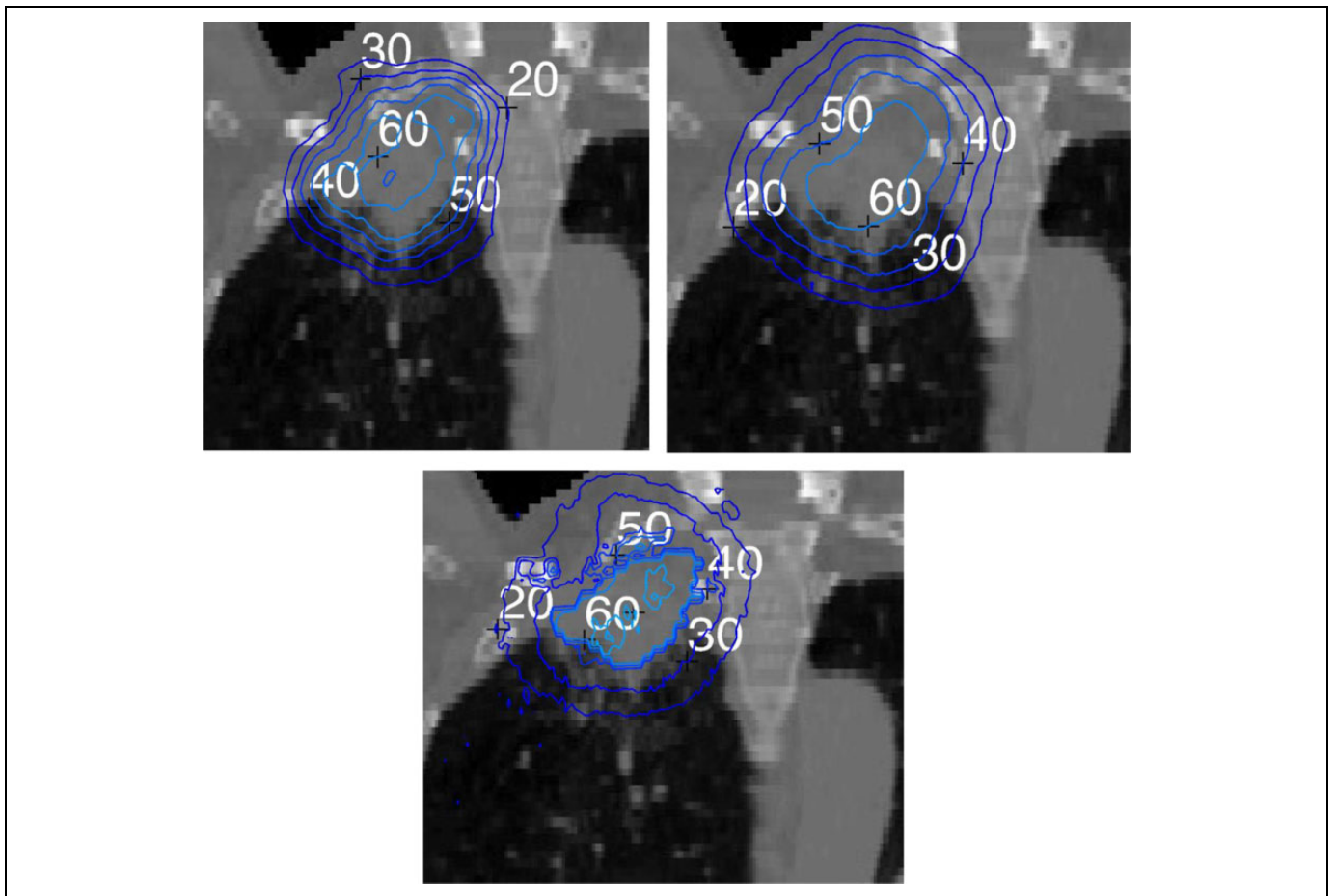

Figure 9. Isodose curves on the coronal plane for the 3 treatments modeled in this work: upper left panel—ideal 6 MV treatment; right panel—imparted 6 MV; bottom panel—imparted contrast-enhanced radiotherapy (CERT).
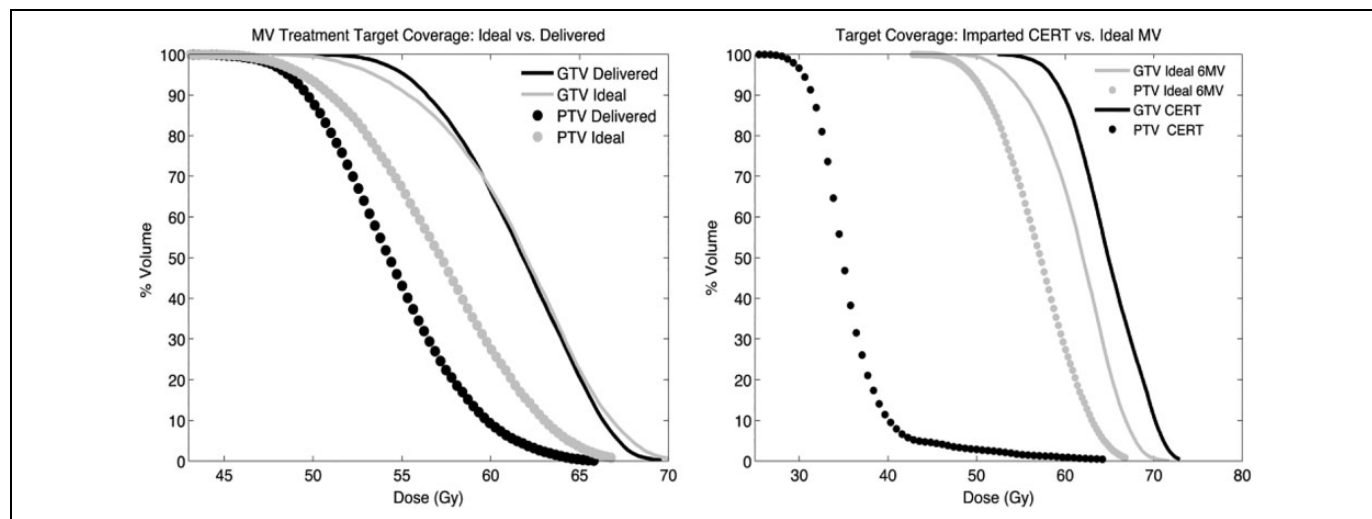
Figure 10. Cumulative dose-volume histogram (cDVHs) for the imparted treatment plans in each of the modalities modeled in this work. Target coverage in each treatment adheres to the recommendations set forth in RTOG 0915.

and CERT imparted. Again, in all 3 treatments, 100% of the GTV receives the prescribed dose of 48 Gy, so the margin as recommended by RTOG 0915 fully compensates for intrafraction motion.

Figure 10 shows the effect that such a motion has on the target coverage for the high-energy and CERT treatments, using the ideal 6-MV plan as the reference. As mentioned before, GTV coverage is excellent independent of the treatment modality and is not affected by the patient motion. For the high-energy treatment, left panel of Figure 10, and unlike in the patient case previously discussed, a larger degradation is seen in the absorbed dose distribution of the PTV when comparing the delivered against the ideal treatment. In spite of this, 97% of the PTV is receiving the prescribed dose of 48 Gy.

As mentioned before, a portion of the ribs is encompassed by the PTV, and while for the megavoltage treatment its presence is not clearly discernible from the resultant cDVH, for the CERT-imparted treatment, right panel in Figure 10, the presence of bone with its high kilovoltage X-ray absorption efficiency results in a distorted cDVH: At least 5% of the PTV volume is now receiving absorbed doses exceeding 40 Gy. From the isodose curves show in Figure 9, however, it is clear that these high doses are being imparted to bone and not to the healthy lung tissue. Moreover, the maximum PTV dose is approximately the same as in the ideal high-energy treatment but with an average PTV dose of 22.5 Gy as opposed to 50.6 Gy for the 6-MV treatment.

Table 5 shows the maximum absorbed doses imparted to at least 1 cm^3 of different OARs, using the recommendations set forth in RTOG 0915. All treatments modeled are within these recommendations. For the lungs, heart, and esophagus, the CERT treatment closely approaches the ideal, static patient and minimum PTV margin, 6-MV treatment. Note again that CERT imparts doses to the skin and bone, not considering the portion inside the PTV, ranging from 30% to 100% above the dose

Table 5. Maximum Absorbed dose (Gy) Imparted to at Least 1 cm^3 of Selected Irradiated Structures.

Structure	Ideal 6 MV	Imparted 6 MV	Imparted CERT	RTOG 0915
Lung	20.0	28.2	20.1	-
Heart	2.9	3.9	2.9	34.0
Trachea	16.4	24.5	27.9	34.8
Esophagus	18.6	25.9	18.5	30.0
Skin	9.4	11.6	18.6	36.0
Ribs	19.7	22.9	25.4	40.0

Abbreviation: CERT, contrast-enhanced radiotherapy; PTV, planning target volume.
[a]Per RTOG 0915, the 2-cm margin around the PTV is not considered.

delivered by the ideal high-energy treatment but still within the safety limits recommended by RTOG 0915.

Figure 11 shows the effect on both the GTV and the PTV of combining the high-energy and CERT-imparted treatments with several weights. For the GTV, as the CERT treatment weight is increased, the average dose also increases, while for the PTV the opposite holds true. From the right panel of Figure 11, it is evident that bone behaves essentially as a contrast agent loaded into the PTV.

Yet, even if only 20% of the prescribed dose is imparted via the CERT modality, the total PTV receiving doses at or above 50 Gy is reduced from 95% down to 40%, despite the inherent patient motion, the large PTV margins and the presence of bone in the margins used in both treatments. Furthermore, as shown on the left panel of Figure 12, at doses near the prescription level, there is an important reduction in the planning volume irradiated even when only one-fifth of the total dose is imparted via the CERT modality. However, the reduction in the volume receiving intermediate doses, central panel in Figure 12, is more modest. This is the dose level, as shown un Figure 10, where absorption by bone prevents the cDVH for the PTV from
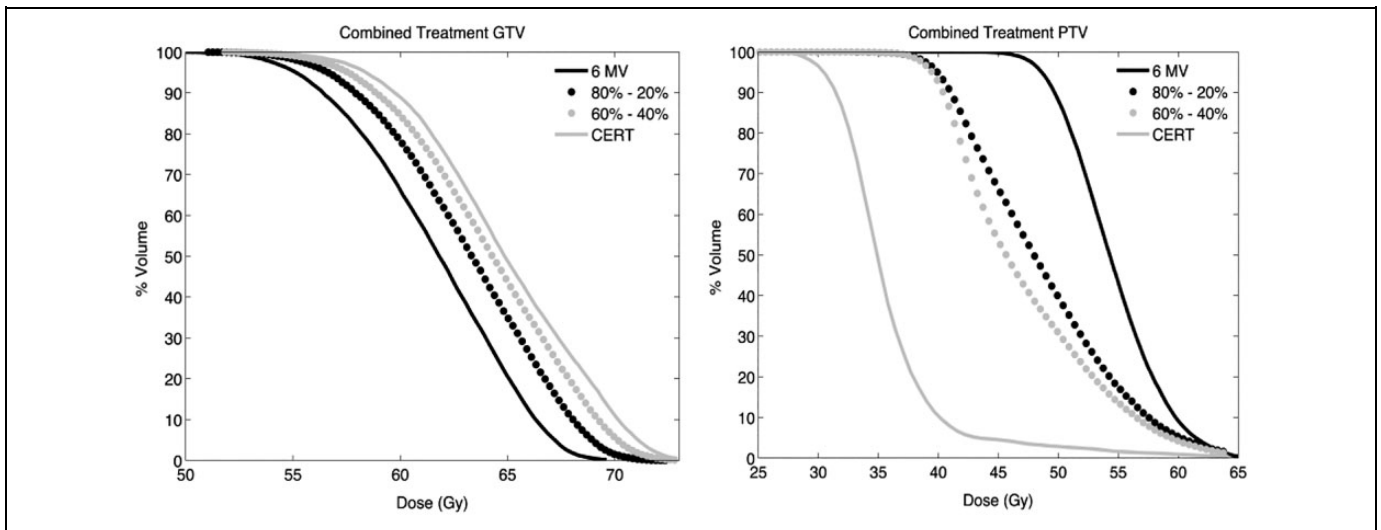
Figure 11. Cumulative dose-volume histogram (cDVHs) for the gross target volume (GTV), right panel, and planning target volume (PTV) for different combination of high-energy and contrast-enhanced radiotherapy (CERT) treatments. Each pair of percentage figures in the labels refer to the weights of the high-energy and the CERT treatments in this order.
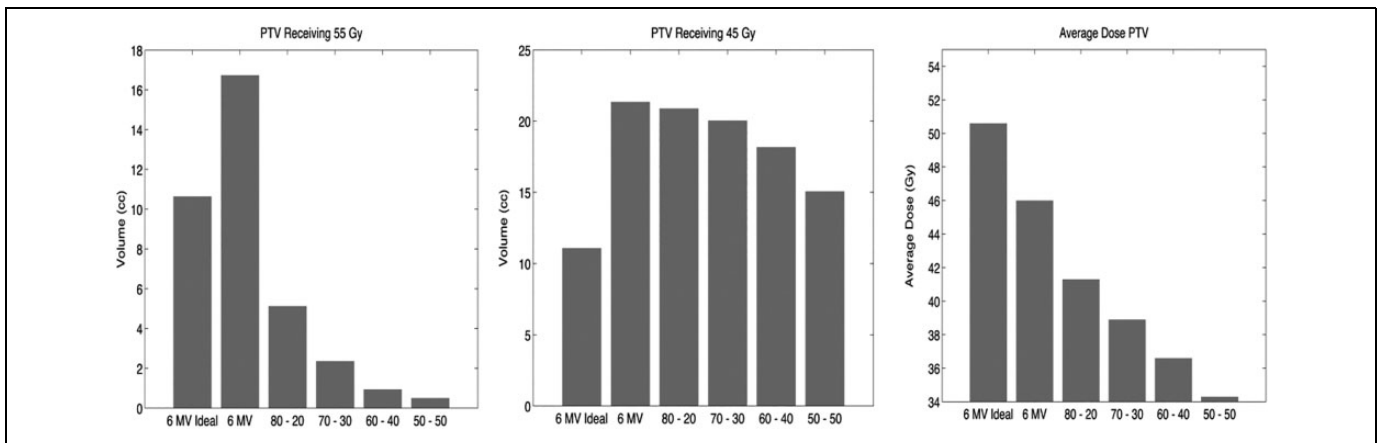

Figure 12. Total planning target volume (PTV) irradiated to at least 55 Gy and 45 Gy and average PTV dose as a function of the percentage of the total dose delivered by each modality

falling to zero as was the case in the centrally located tumor. Note however that the average PTV dose, right panel of Figure 11, decreases by at least 10% when the total dose is split between the 6-MV and CERT modalities at a ratio of 80% to 20%, with even larger reductions for other ratios.

Figure 13 shows both the lung, outside the 2-cm margin defined by RTOG 0915, and the esophagus volume receiving at least 15 Gy and 10 Gy, respectively. For the lung tissue in particular, the reduction in volume is not as pronounced as for the centrally located tumor because, as mentioned before, the PTV encompasses not only the lung but a sizable portion of other tissues. The esophagus does exhibit a reduction of almost 30% in the volume receiving at least 10 Gy when the 6 MV and CERT modalities are combined with different ratios.

As noted in the centrally located tumor, the absorbed dose imparted to both the skin and the ribs, shown in Figure 14, increases as the percentage of total dose imparted via the CERT

modality increases, which as discussed before is a consequence of the physical characteristics of the absorption process undergone by kilovoltage X-ray beams. It is important to emphasize that according to Table 5, the tolerances established by RTOG 0915 are never exceeded.

Discussion

There already exists clinical experience related to the irradiation method proposed in this work: a phase I study to evaluate the use of a CT scanner for the treatment of metastatic brain tumors upon which an iodinated contrast agent had been previously loaded was carried out without adverse reactions observed, with treatments imparted with a combination of megavoltage and CERT modalities.[23] Remarkably, some of the irradiated tumors vanished after 4 treatments. While in the aforementioned trial the PTV margin did not play a role as the
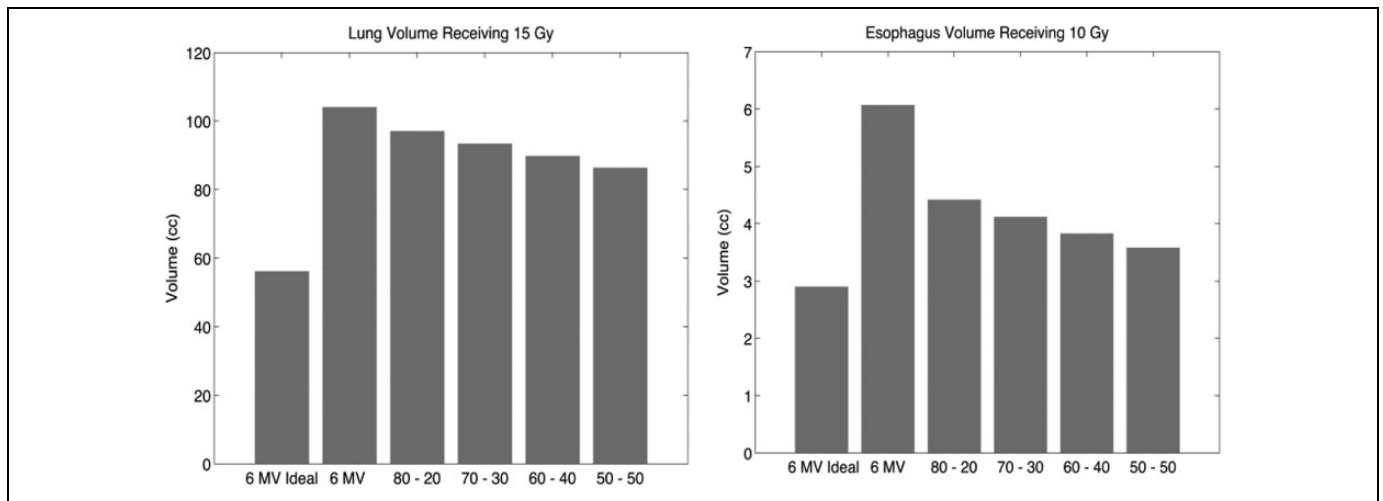
Figure 13. Left panel: total volume of lung receiving at least 15 Gy (both lungs); right panel: volume of the esophagus irradiated to at least 10 Gy.
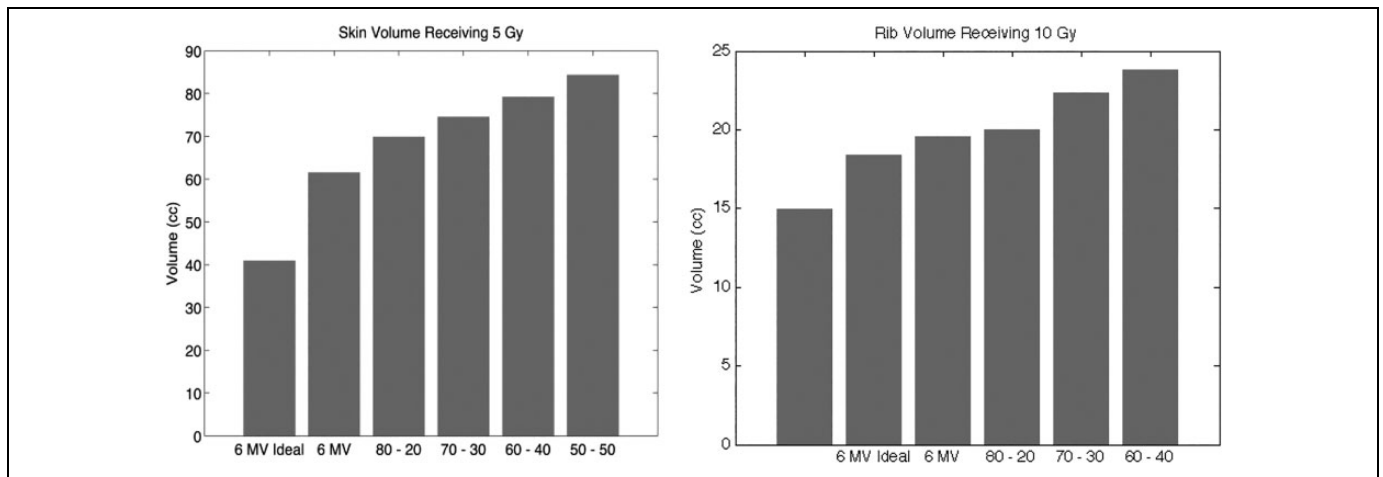

Figure 14. Volumes of skin and ribs irradiated to 5 Gy and 10 Gy, respectively.

whole brain was being irradiated, in this work, we have shown an additional advantage of combining megavoltage and CERT therapies: Its robustness against intrafraction motion as the only restriction placed on the PTV margin would be that it needs to be large enough to fully encompass the motion amplitude of the GTV to be irradiated and thus resulting in absorbed dose distributions that closely follow what would be obtained under ideal conditions.

While it has been shown that the presence of bone inside the relatively high-dose PTV region does not adversely affect GTV coverage in CERT treatments, see Figure 10, the presence of air pockets or low-density tissue and the ensuing disruption of charged particle equilibrium must also be considered. We argue that for kilovoltage X-ray beams, for which the secondary electron field has ranges in the order of micrometers, the presence of low-density tissue or air pockets, particularly in the periphery of the tumor, should not be as detrimental for the overall treatment plan as it is for the megavoltage beams.

From a radiobiological perspective, we have recently shown that kilovoltage and megavoltage robotic SBRT for lung result in differences of less than 5% in the tumor control probability (TCP) and normal tissue complication probability (NTCP),[13] although it is likely that the presence of the contrast agent embedded in the tumor, not present in the referenced work, would change its biological response to kilovoltage X-ray beams. This change, in principle, would be beneficial in terms of the TCP as the high linear energy transfer of the electron cascade released from the high-atomic number atoms in the contrast agent would result in an increased lethality.[24] As the radiobiological parameters needed to account for the presence of the contrast agent in the GTV are not known, it is not possible to estimate the TCP for the treatment plans modeled in this work. We have shown, however, that when combining high-energy and CERT treatments, the OARs are receiving even lower maximum doses than when no contrast agent was used as part of the treatment. Based on these findings, we

believe that it is reasonable to expect an even lower NTCP for CERT, perhaps on par with what it is usually obtained for megavoltage treatments.

One critical aspect of the proposed approach, and of CERT in general, is the specificity with which the GNPs would predominantly accumulate in the tumor and not the healthy tissue surrounding it. It is clear that conventional iodine-based contrast agent do accumulate preferentially in the tumor tissue[23] which is important as the higher the specificity, the greater the difference between the absorbed dose in the tumor and that of the surrounding tissue. While in this type of contrast agent there is not much room for improving the specificity, nanoparticle-based agents, through the optimization of the nanoparticle size, do offer this possibility. While experimental data with mice seem to indicate that 2 nm in diameter GNP offers excellent specificity,[6] in humans, the average pore size of healthy and tumor tissue vasculature, 60 nm and 240 nm, respectively, suggests that GNP with diameter in the order of 100 nm would be better suited for the purpose of CERT.[25]

Several logistic aspects of the proposed method related to the treatment-planning process would have to be addressed. In particular:

1. Quantification of the contrast agent concentration in the tumor: This is important as the absorption of kilovoltage X-rays, and therefore the total dose imparted, depends on the amount of contrast agent present at a given point in the patient. This in principle should not represent a serious impediment to the proposed method, as the measurement of the contrast agent concentration can be carried out using the same set of CT images used for treatment-planning purposes, provided that a suitable calibration curve has been previously obtained[26] and, of course, that the contrast agent was administered prior to the CT scanning process.

2. Variation in the contrast agent concentration with time: This is by far the most challenging problem associated with the proposed method and in general to the CERT modality. For the particular case of GNP-based contrast agent, it has been reported that, in mice, the concentration of GNP in the tumor reaches a plateau at about 5 hours postinjection and stays fairly constant for periods of up to 24 hours,[27] with clearance from other tissues and organs at a much faster rate. It is not clear from this study how the concentration changes 24 hours after the administration. Therefore, for a single fraction treatment, as in robotic SBRT, variation in contrast agent concentration with time should not be a problem, as the treatment session usually lasts between 30 and 90 minutes. For multifraction SBRT, further research would be needed regarding the dynamics of the GNP in the tumor for time periods of at least 1 week postadministration, in order to determine whether additional administration of the GNP would be needed

From a technological perspective, it has been assumed in this work that a robotic therapy machine capable of dual mega- and kilovoltage X-ray beam generation is used to deliver the treatment. While this technology is not currently available in the clinic, its main components are already present in the treatment room. There are 2 possibilities to obtain the kilovoltage X-ray beam needed to carry out the irradiation as modeled in this work:

1. Target material and geometry optimization such that the megavoltage incident electron beam yields a sizable component of kilovoltage X-rays that could then be used for the purposes of CERT irradiation. This approach has been pursued in the context of portal imaging,[28,29] with the obvious disadvantage that it would be impossible to independently control the kilovoltage beam quality and output rate.

2. On linac with a gantry-mounted X-ray tube intended for tumor tracking, repurposing such an X-ray tube in order to obtain the desired spectrum and beam output may be an option. Note that this is not exactly what was modeled in this work, as we assumed that both the kilovoltage and the megavoltage beams are aimed from the same position and with the same direction. However, in light of the results presented in this work, it is reasonable to conclude that using the already available X-ray tube is a viable alternative to the proposed method

We believe a third option that could be implemented in the linacs used in the CyberKnife systems, as they do not have a flattening filter and bending magnet, would be to independently accelerate, via DC voltage, a separate electron beam and use the same target, with a slight modification, to generate both the high- and low-energy beams. This would allow to independently manipulate the dose contribution from CERT as deemed fit and also to fine-tune the kilovoltage X-ray spectra to the particular characteristics of the target to be irradiated. This approach is currently under theoretical analysis at our laboratory, particularly with regard to the cooling system necessary to dissipate the extra heat generated in the target material due to the additional electron beam incident on it and also with regard to the characteristics of the resultant kilovoltage X-ray beam.

ORCID iD

Héctor M. Garnica-Garza https://orcid.org/0000-0002-9800-4856

References

1. Brandner ED, Chetty JJ, Gladdui TG, Xiao Y, Huq MS. Motion management strategies and technical issues associated with stereotactic body radiotherapy of thoracic and upper abdominal tumors: a review from NRG oncology. *Med Phys*. 2017;44(6):2595-2612.

2. Freislederer P, Reiner M, Hoischen W, et al. Characteristics of gated treatment using an optical surface imaging and gating system on an Elekta linac. *Radiat Oncol*. 2015;10:68.

3. Adler JR, Chang SD, Murphy MJ, Doty J, Geis P, Hancock SL. The Cyberknife: a frameless robotic system for radiosurgery. *Stereotact Funct Neurosurg*. 1997;69(1-4 pt 2):124-128.

4. Poulsen PR, Cho B, Langen K, Kupelian P, Keall P J. Three dimensional prostate position estimation with a single x-ray imager utilizing the spatial probability density. *Phys Med Biol*. 2008;53(16):4331-4353.

5. Poulsen PR, Cho B, Keall PJ. Real time prostate trajectory estimation with a single imager in arc radiotherapy: a simulation study. *Phys Med Biol*. 2009;54(13):4019-4035.

6. Hainfeld JF, Slatkin DN, Smilowitz HM. The use of gold nanoparticles to enhance radiotherapy in mice. *Phys Med Biol*. 2004;49(18):N3019-N315.

7. Garnica-Garza HM. Contrast-enhanced radiotherapy: feasibility and characteristics of the physical absorbed dose distribution for deep seated tumors. *Phys Med Biol*. 2009;54(18):5411-54255.

8. Clark K, Vendt B, Smith K, et al. The cancer imaging archive (TCIA): maintaining and operating a public information repository. *J Digit Imaging*. 2013;26(6):1045-1057.

9. Hugo GD, Weiss E, Sleeman WC, et al. Data from 4D lung imaging of NSCLC patients. *Cancer Imaging Arch*. 2016. doi:org/10.7937/K9/TCIA.2016.ELN8YGLE.

10. Hugo GD, Weiss E, Sleeman WC, et al. A longitudinal four-dimensional computed tomography and cone beam computed tomography dataset for image-guided radiation therapy research in lung cancer. *Med Phys*. 2017;44(2):762-771.

11. RTOG 0813. Seamless Phase I/II Study of Stereotactic Lung Radiotherapy (SBRT) for Early Stage, Centrally Located, Non-Small Cell Lung Cancer (NSCLC) in Medically Inoperable Patients. 2011. https://www.rtog.org/ClinicalTrials/ProtocolTable/StudyDetails.aspx?study=0813.

12. RTOG 0915. A Randomized Phase II Study Comparing Two Stereotactic Body Radiation Therapy (SBRT) Schedules for Medically Inoperable Patients with Stage I Peripheral Non-Small Cell Lung Cancer. 2014. https://www.rtog.org/ClinicalTrials/ProtocolTable/StudyDetails.aspx?study=0915.

13. Sánchez-Arreola SV, Garnica-Garza HM. Feasibility of robotic stereotactic body radiotherapy of lung tumors with kilovoltage x-ray beams. *Med Phys*. 2017;44(4):1224-1233.

14. Cimmino G. Calcolo approssimato per le soluzione dei sistemi di equazione lineari. La Ricerca Scientifica. 1938;1938 Roma XVI Ser. II, Anno IX 1 326-333.

15. Censor Y, Altschuler MD, Powlis WD. On the use of Cimmino's simultaneous projection method for computing a solution of the inverse problem in radiation therapy treatment planning. *Inverse Problems* 1988;4(3):607-623.

16. Vanderstraeten B, Chin PW, Fix M, et al. Conversion of CT numbers into tissue parameters for Monte Carlo dose calculations: a multi-centre study. *Phys Med Biol*. 2007;52(3):539-562.

17. Mesa AV, Norman A, Demarco JJ, Smathers JB. Dose distributions using kilovoltage x-rays and dose enhancement from iodine contrast agents. *Phys Med Biol*. 1999;44(8):1955-1968.

18. Salvat F, Fernández-Varea JM, Sempau J. PENELOPE-2006: a Code System for Monte Carlo Simulations of Electron and Photon Transport Nuclear Energy Agency (OECD) Workshop Proc; July 2006; Barcelona, Spain.

19. Sempau J. PENEASY, a structured main program from PENELOPE. Barcelona; 2006. http://www.upc.es/inte/downloads/penEasy.htmv.2006-06-01ed. Accessed October 14, 2019.

20. Sechopoulos I, Rogers DWO, Bazalova-Carter M, et al. RECORDS: improved Reporting of montE CarlO RaDiation transport Studies: report of the AAPM research committee task group 268. *Med Phys*. 2018;45(1):e1-e5.

21. Francescon P, Cora S, Cavedon C. Total scatter factors of small beams: a mutidetector and Monte Carlo study. *Med Phys*. 2008;35(2):504-513.

22. Garnica-Garza HM. Treatment planning considerations in contrast-enhanced radiotherapy: energy and beam aperture optimization. *Phys Med Biol*. 2011;56(2):341-355.

23. Rose JH, Norman A, Ingram M, Aoki C, Solberg T, Mesa A. First radiotherapy of human metastatic brain tumors delivered by a computerized tomography scanner (CTRx). *Int J Radiat Oncol Biol Phys*. 1999;45(5):1127-1132.

24. Garnica-Garza HM. Microdosimetry of x-ray-irradiated gold nanoparticles. *Radiat Prot Dosimetry*. 2013;155(1):59-63.

25. Fullstone G, Wood J, Holcombe M, Battaglia G. Modelling the transport of nanoparticles under blood flow using an agent-based approach. *Sci Rep*. 2015;10:10649.

26. Garnica-Garza HM. Apparatus and method to carry out image-guided radiotherapy with kilovoltage x-ray beams in the presence of a contrast agent. United States Patent 8681937B. 2014.

27. Liu J, Yu M, Zhou C, Yang S, Ning X, Zheng J. Passive tumor targeting of renal-clearable luminescent gold nanoparticles: long tumor retention and fast normal tissue clearance. *J Am Chem Soc*. 2013;135(13);4978-4981.

28. Flampouri S, Evans PM, Verhaegen F, Nahum AE, Spezi E, Partridge M. Optimization of accelerator target and detector for portal imaging using Monte Carlo simulation and experiment. *Phys Med Biol*. 2002;47(18):3331-3349.

29. Parsons D, Robar JL, Sawkey D. A Monte Carlo investigaton of low-Z target image quality generated in a linear accelerator using Varian's VirtualLinac. *Med Phys*. 2014;41(2):021719.